Location-Aware Augmented-Reality for Predicting Sea Level Rise in Situ

Froso Sarri
Information Management Systems Institute
Athena Research Center
Athens, Greece
frososarri@athenarc.gr

Lemonia Ragia
Information Management Systems Institute
Athena Research Center
Athens, Greece
leragia@athenarc.gr

Antigoni Panagiotopoulou
Information Management Systems Institute
Athena Research Center
Athens, Greece
antigoni27aug@gmail.com

Katerina Mania
School of Electrical and Computer Engineering
Technical University of Crete
Chania, Greece
amania@isc.tuc.gr

2022 International Conference on Interactive Media, Smart Systems and Emerging Technologies (IMET) | 978-1-6654-7016-2/22/$31.00 ©2022 IEEE | DOI: 10.1109/IMET54801.2022.9929635

***Abstract*—Public awareness of climate change's growing impact on coastal areas is vital for assessing and managing future environmental changes in order to restrain its effect. Accessibility to climate change data and evident display of its consequences can promote social engagement. Augmented Reality (AR) technology can efficiently communicate scientific data, advocating the environmental message. However, AR comes with usability and interaction challenges especially outdoors inbright sun light, noise and traffic. This paper presents a location-aware, interactive visualization of the predicted sea level rise on the coastal area of the old city of Chania in Crete, Greece. Usability challenges in relation to AR operating outdoors are tackled in relation to non-obstructive virtual content placement and interaction, while the integration of external GPS data enable accurate geolocation. An interactive system enables the user to witness the sea level rise impact on site, in real-time, up to the year 2100 prompting immediate awareness of future environmental changes and associated hazards.**

***Index Terms*—Augmented Reality; GPS; Microsoft Hololens; Sea Level Rise; Mediterannean Coastal Database; Climate Change; Modelling and Visualization**

I. Introduction

Augmented Reality (AR) allows the integration of the physical world with digital information [37] [38] for navigation aids, geological mapping, visualization of climate change effects among others application areas [12], [35], [36], [43]. AR-enabled devices can put on view virtual holograms while users also see the real world, performing satisfactorily accurate spatial mapping without extra hardware [14]. Apart from AR on mobile phones or tablets, head-mounted AR glasses are intuitive offering hands-free interaction [13] [15], [26]. Although head-worn AR devices were mostly purposed for indoor usage, outdoor operation is shown to be challenging in relation to spatial mapping as well as interactivity, while a user is on the move in busy, bright and noisy outdoor spaces [41], [42].

Leveraging the capabilities of AR head-worn devices, this paper proposes an interactive geo-located visualization system operating outdoors, in real-time. The system advocates the impact of environmental changes on a coastal area by visualizing coastal erosion as predicted by environmental data in the specified by the user time point, up to 2100. Future estimations of sea level rise (SLR) data are extracted through regionalized SLR scenarios, rendered and visualized based on AR technology. The implemented system is used on site and utilizes the AR device's spatial capabilities integrating externally sourced position tracking via GPS data integration, in our case, via an Android smartphone. The interactive system enables the user to visualize the predicted sea level rise and the consequent impact on the coastal area of the historic centre of Chania, Crete, Greece. The system provides geospatial information for the accurate placement of the water simulations as rendered in 3D to coincide and extend the existing sea level, facilitating intuitive navigation features. The merging of real and virtual environments through the demonstration of the SLR phenomenon enables users to comprehend climate change and witness its impact in situ.

II. Related Work

A. AR data visualization in situ

Modelling and visualizing 3D geographic scenes with timely data in physical space has provided users with 3D geographic information in relation to environmental phenomena such as coastal erosion [53], [25], [18]. In-situ data presentation in the real world can be of great benefit for public awareness of environmental issues. An AR application named HypAR has empowered in-situ inspection of mineralogy, spatially co-located and embedded with rock surfaces [17]. An MR tornado simulator enables students and the instructor to collaborate aiming to inform about tornado formation and its harmful effects on human-built structures, on farming as well as on vegetation [10]. Visualization of future predictions is playing crucial role in awareness of environmental changes [44].

Demonstration of scientific data in-situ based on AR does come with technical and usability challenges of enabling

efficient human navigation as well as accurate spatial mapping and registration of digital information outdoors, either in urban or countryside settings. Previous work on AR navigation focuses on indoor environmental conditions by presenting virtual semantic landmarks in aid of spatial knowledge acquisition [29]. Holographic 3D visual stimuli is used for training in evacuation [48]. Spatial knowledge of outdoors environmental settings cannot be based on virtual semantic indicators as when AR systems operate indoors, due to the volatility of urban areas and the inaccuracy of the positional arrangement. The spatial knowledge acquisition of an outdoors system needs to be independent of semantic content (virtual of physical) and should rely on outsourced geo-location information. Previous approaches achieve outdoors position tracking with the aid of external devices such as the real-time kinematic global navigation satellite systems (RTK GNSS) units [28], the radio frequency identification (RFID) set ups including tags and receivers [56] or via commercial GPS sensors [23]. Such multiple-component based systems are complex and the employed hardware is not commonly accessible. The integration of geographic data on a simplified system optimizes the positioning of virtual objects in the physical environment aligned with user expectations [21], [46]. Easy hardware access and design simplicity guide our proposed system design.

B. Climate Change and Sea Level Rise

Enhanced greenhouse effects have caused global climate change while adaptation policies in concern to climate change effects is needed [9], [34], [40], [45]. For the time period between 1870 and 2004, there was a rise at the Sea Level (SL) of average rate 1.7 mm±0.3 mm/year where in the last 10 years the rate increased significantly [11]. Thermal expansion of sea water, caused by temperature increment of the ocean upper layer, is defined as the key source of SLR [47]. Thereafter, the upsurge of SL is an enduring thermodynamic process resulting from the ocean and upper ocean regions being affected by climate change [55]. SLR is expected to have a tremendous impact on human activity near coastal regions. Actually, inundation of low-lying coastal areas constitutes a long-term problem having been under consideration in a broad range of different fields [6]. SLR of 0.57–1.10 m by 2100 has been predicted as medians from 2,000,000 runs [24]. SL will keep rising for many centuries after stabilization of radiative forcing, finally outstretching to 1.84–5.48 m by 2500, excluding the RCP3PD low emission scenario. On a global scale, the projected mean SLR for the future was calculated at 0.27m, whilst for East Asia the SLR was a bit smaller. The coastal flood damage and adaptation costs under 21st century SLR is assessed by considering a broad range of uncertainties regarding population data, continental topography data, protection strategies, socioeconomic development and SLR [22]. In absence of adaptation, 0.2-4.6% of the global population is anticipated to be flooded annually in 2100 under 25-123 cm of global mean SLR. Moreover, with concern to coastal SL changes and the associated risks of flooding as well as erosion, wind waves are a dominant factor [30].

Future climate projections are feasible through global climate models. Uncertainties as well as assumptions about future greenhouse gas emissions, i.e. Representative Concentration Pathways-RCPs, are contained whilst the extent of Greenland and Antarctica ice melt and consequently SLR, are modeled [20]. Predictions regarding the next few decades overall agree but in concern with year 2100, they differ. Values for the end-of-century (2100) range from a low of $\sim$ 50 cm to as high as $\sim$310 cm. [16]. SLR will not stop at 2100 but will continue for even centuries and millennia, following emissions stopping. By 2100, GMSL (Global Mean Sea Level) is projected to increase by 0.28–0.55 m under SSP1-1.9 (shared socioeconomic pathway) and per 0.63–1.02 m under SSP5-8.5 relative to the 1995–2014 average [6]. Ice-sheet processes, that are typified by deep unpredictability, could lead GMSL rise up to about 5 m by 2150. Regional SL changes present differences in comparison with global estimates [19], [50]. Over the 21st century, most coastal locations present a median projected regional SLR within ± 20% of the projected GMSL change [6]. Approximately 66m of potential SLR are contained in the ice sheets and glaciers of Antarctica, Greenland and the mountain glaciers of the planet [4]. In the current century, an SLR of just 1m will cause negative effects for developed shorelines around the globe. Roughly 110 million people live below the present high tide today and 250 million occupy land below current annual flood levels [27]. Public awareness of SLR and climate change visualized in situ is of paramount importance so that appropriate remedial action is initiated.

III. System Design and Implementation

Wearing the head-worn AR device, the user is able to activate the 3D simulation of sea level rise in situ.

A. Sea Level Rise Predictions

The study focuses on three geographical locations along the coastal area of Chania. For this particular region, coastal data are available through the Mediterranean Coastal Database (MCD) [7], [36], [39], [54]. Regionalized SLR scenarios have been formulated that consider changes due to ocean temperature and salinity variations. Mean SLR relative to 1985-2005 in meters for RCP values equal to 2.6, 4.5 and 8.5 for a high ice-sheet melting scenario and for a medium ice-sheet melting scenario are available [22]. Despite the fact that the latter study gives results being equal in range to the ones presented in national studies [33], certain uncertainties remain which are deep-rooted to the character of the global socioeconomic coastal analysis. Furthermore, the groundwater depletion for human usages, which was estimated to commit up to around 8 cm to global SLR by the end of the century [52] is maltreated in [22]. Likely storminess changes and potential rise in cyclone intensity, together with SLR, could change flood damage [24] but are not considered here. An extra key element of uncertainty is human effected subsidence which is brought about from the withdrawal of ground fluids. The latter may lead to rates of local relative SLR that supersede per one order of magnitude the current rates of climate-induced global-mean

SLR [49]. Table I presents the mean SLR values in meters, as provided by the MCD. The three geographical points under consideration are assigned just about the same mean SLR [54]. Regarding all three RCP values, two characteristic trends can be discerned a) the mean SLR increases during the years from 2025 to 2100 b) the high ice-sheet melting scenario values exceed those of the medium scenario [22].

TABLE I: Mean SLR in meters for RCP 2.6, 4.5 and 8.5 [22].

	RCP26		RCP45		RCP85	
Year	**M[1]**	**H[2]**	**M**	**H**	**M**	**H**
2025	0.079	0.110	0.080	0.111	0.086	0.124
2030	0.101	0.145	0.100	0.140	0.108	0.154
2035	0.121	0.174	0.119	0.168	0.134	0.190
2040	0.138	0.200	0.141	0.202	0.156	0.227
2045	0.156	0.228	0.164	0.236	0.188	0.268
2050	0.178	0.260	0.190	0.275	0.221	0.317
2055	0.197	0.288	0.218	0.317	0.255	0.371
2060	0.215	0.318	0.246	0.361	0.295	0.434
2065	0.232	0.345	0.276	0.410	0.336	0.499
2070	0.250	0.374	0.306	0.461	0.381	0.568
2075	0.267	0.402	0.337	0.510	0.426	0.639
2080	0.284	0.429	0.368	0.557	0.475	0.718
2085	0.302	0.458	0.397	0.604	0.528	0.803
2090	0.320	0.486	0.428	0.651	0.583	0.893
2095	0.338	0.513	0.457	0.698	0.638	0.988
2100	0.356	0.542	0.487	0.746	0.696	1.090

[1] Medium Scenario, [2] High Scenario.

B. System Requirements and Limitations

The AR visualization system proposed is designed to be aware of the user's position achieving the water simulation realism and accurate integration of the water simulation with the real-world coastal edge. The constant flow of geographical information to the system designates the Hololens 2 AR device spatially and geographically aware. Our objective of AR SLR visualization generates the following requirements: 1) establishing the device for outdoor use, 2) achieving accurate spatial placement of user and virtual content, 3) developing a ubiquitous system and a flexible application independent of spatial anchoring, 4) enhancing usability in relation to the interaction between a user and holographic content, 5) optimizing system performance in real time. A common attribute of head-worn AR devices is the lack of GPS receiver, leading us to acquire location data from an external source, e.g. a smartphone.

C. System Design

We decided to incorporate a standard device such as a smartphone or tablet as a GPS receiver. The accessibility of those devices and their ubiquitous location services constitute a solid source of the geographical data needed for the system implementation. We developed a system that consists of two components; the AR application implemented for the Hololens 2 device visualizing SLR at the coastal area of the historical centre of Chania and the mobile application, developed for Android devices, which provides the GPS data to geographically and spatially position the digital information of water simulation included in the AR system. The two components are connected through a WiFi network, via which the geographic data will be transmitted (Fig. 1). While on site, the user will launch both the AR visualization system and the mobile application. The two devices must be connected to the same WiFi network in order to communicate. GPS data are transmitted from the Android to the AR system, as an alternate location service module. The system is designed to continuously provide GPS location tracking. This drives the accurate placement of the simulated holograms in the physical environment, while also facilitating the implementation of navigation services operating on the Hololens device.

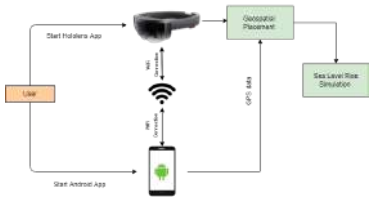

Fig. 1: An overview of the system design.

D. GPS Data Integration

The communication between the devices is achieved by utilizing the principles of the Transmission Control Protocol (TCP). In a server-client based schema, data are transmitted through a local network using sockets. The Android application acts as the server, while the AR system as the client. The Android app creates a TCP server and waits for client connections in a particular port via a TCP listener. When a client is identified in the network, a connection with the server is established and the transmission begins. The configuration of the connection is attained via the server's IP address. The user includes the server's IP address, i.e the IP of the Android device, in the AR system via the Hololens 2 device.

The message broadcast through the connection contains data about the geographical location of the mobile device. Latitude, longitude and orientation readings are continuously relayed through the server. The application accesses the device's native location service functionality to retrieve the latitude and longitude position values. Studies have shown that about 95% of the time, smartphone devices are accurate within 10 meters [31]. Further research has indicated that smartphone GPS receivers are considered to have a median error of 5 - 8.5 meters [57]. Recently, the horizontal position error of mobile smartphones was calculated to be in the 7-13 meter range [32]. Environmental and atmospheric conditions affect GPS accuracy. Dense infrastructure in urban areas worsens it, while the GPS-enabled smartphones are typically accurate to within a 4.9 m radius under open sky [51]. Taking into account the size of the water volumes to be visualized, the general margin of error is considered acceptable for the proposed development. The Android device's heading values compensate for the lack of surface compass reading measurements on the Hololens device. Although Hololens devices are equipped with gyroscope and magnetometer, these are used to determine

rotations and estimate absolute orientation of the device itself, i.e. the head orientation in local space. The measured heading values derived from the phone are sent through the connection, in order to synchronize the Hololens 2 head tracking with the actual heading direction relative to the geographical north pole. A calibration process, that offers compass capabilities to the Hololens 2 device was developed. The transmitted data were constantly updated according to the Android device's sensor measurements. The application dynamically informs the user of the current server and connection status and provides the ability to restart the server for troubleshooting purposes.

E. AR system

The main AR system focuses on the visualization of the SLR on site. SLR is simulated on three spots across the old harbor of the city of Chania. The users are guided to each one of them and once they arrive at each spot, they can activate the simulation. A 3D hologram of the water is displayed according to the SLR model data and SLR predictions, simulated from year 2050 to 2100. The 3D object that represents water utilizes Unity's Universal Render Pipeline (URP) system and attains its authenticity with a realistic water shader built in Unity's Shader Graph tool. The created shader sets and handles color, depth, wave and surface transparency levels, enhancing its realism. Upon launch, the AR system (Hololens 2 acting as a client) connects with the server (Android device) and receives GPS and orientation data for its geospatial placement. The connection is maintained throughout the use of the app.

Calibration: The user orientation in the physical environment does not correspond with the AR device's inertial measurement unit when the application is launched. In order to configure geographical tracking, a calibration process is performed at the start. A 'pointer' 3D object is presented in front of the user which is aligned with the AR device's virtual coordinate system in the zero vector direction. The user is instructed to place the phone on the pointer object and the heading direction of the phone is recorded through the TCP connection (Fig. 2a). The recorded value is considered the deviation between the AR device's orientation and the actual north direction. The pointer object is then rotated according to this deviation. To facilitate the calibration, the user is suggested to face the new pointer direction (Fig. 2b). A procedure is then initiated while the tracking features of the AR device's are centered to the current position and orientation of the user. Upon finishing, the geographic coordinate system and the device's coordinate system are aligned, providing actual geographical tracking in the AR device. The development of navigational aids such as the inclusion of compass characteristics in the system is simplified with the newly established geographical-enhanced orientation, without having to rely on phone's heading readings anymore. This procedure is performed only once, since the AR device's inertial measurement unit maintains tracking of loss events, which is a state the Hololens 2 enters when it can't locate itself in the physical environment. Once tracking is regained, the AR device continues to recognize the real world actual heading orientation and combined with the GPS integration, maintains its geographical awareness.

(a) (b)

Fig. 2: Calibration process: (**a**) Phone placed on the pointer object to record its heading direction. (**b**) The pointer object is rotated accordingly facing the north direction.

Navigation Service: To effectively guide the user to the simulation spots, a navigation help feature can be enabled. It is implemented by utilizing Microsoft's Maps SDK, which integrates mapping in Unity [3]. Maps SDK handles streaming and rendering of 3D terrain data while being optimized for AR applications. The map rendering is configured by Bing Maps [1] based on geolocation input, i.e. latitude and longitude coordinates. A 3D map of the area is placed in front of the user with the simulation spots marked with 3D pins (Fig. 3). The user can press each one of them and information about the distance between the pressed pin, i.e. simulation spot and the current location of the user is displayed. Since distance information must be based on optimized walking routes, Bing Maps REST Services API [2] is utilized to retrieve this content by constructing the appropriate URL. The URL is sent via web request and returns an XML object from which the walking travel distance data from the shortest route graph are recovered. The user's position is constantly displayed on the map. This is achieved by superimposing a geolocation data layer on the map, in which the GPS data retrieved from the TCP connection are rendered, as a 3D pin in the corresponding geolocation on the map.

Fig. 3: 3D navigation map, red pins: simulation spots, green arrow: user's location. Pressing pin no 2 displays user's distance.

Notification System and Relative User Position: A notification system is developed informing the user about entering or leaving a simulation spot. When the users approach one of the three simulation areas, a 3D message panel appears in front of them informing them about which one of the 3 areas they have entered (Fig. 4a). When they attempt to leave a

simulation area, a similar 3D panel appears informing them accordingly (Fig. 4b). The Haversine formula using latitude and longitude data to compute the distance between two points is utilized for constant linear distance calculations between the user's current position derived from the transmitted GPS data and the position of each one of the 3 simulation areas [8]. The users are alerted when they enter a 20 meter radius area around each spot. When the users' position is calculated to be between the 20 meter radius area and a 40 meter radius area from each spot, a message informs that there are no more simulation data beyond their position. Moving beyond that point, halts the simulation altogether.

(a) (b)

Fig. 4: Notification panels for the user's relative position to the simulation areas. Upon: (**a**) entering, (**b**) leaving.

Spatial Mapping and Scanning Configuration: Hololens' spatial awareness facilitates the integration of holograms in the physical environment. Spatial mapping retrieves the geometry of the environment around the device as meshes and the surface data are used for placement and occlusion of the simulated water. The device scans the space its camera points at, e.g., the mapped area is constantly expanded as the field of view changes. The thorough spatial mapping of the simulation area determines coherent interactions and object behaviors. Our aim is the physical environment of the simulation area to occlude the water object for an immersive representation of the SLR impact on the coast line. Fig. 5 shows the occlusion effect which greatly enhances photorealism. Upon entering each area, the user scans the space around them retrieving the surface mesh (Fig. 6). The generated mesh accurately occludes the simulated water object which obtains surface characteristics provided by the water shader. A powerful advantage of head-worn AR devices such as the Hololens 2 is that mapping data are saved on the device and persists across application and device restarts. Hololens 2 constantly updates and refines the spatial mapping based on new data, e.g. the scanned spatial mesh is refined with each use, realistically merging the simulated water object with the physical environment.

SLR Simulation: The user can activate and control the SLR simulation visualizing the sea rise predictions. The predictions are based on RCP values and consider variances for high or medium ice-sheet melting scenarios. Sea level rise estimations per year are taken into account. In future work, the hourly tide height changes could also be taken into consideration. A settings panel is displayed and the user can select between RCP of 2.6, 4.5 and 8.5 as well as between a high melting and a medium melting ice sheet scenario. The simulation can be enabled or disabled. The system takes the input values from the

(a) (b)

Fig. 5: Realistic virtual water occlusion with physical objects: (**a**) A boulder on the pier. (**b**) A pillar.

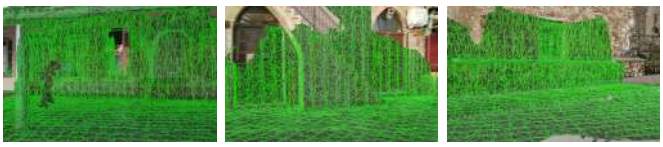

(a) (b) (c)

Fig. 6: The scanned space for hologram occlusion. Simulation areas: (**a**) 1, (**b**) 2, (**c**) 3.

panel and generates as output the calculated SLR predictions. The visualization of the water level is controlled by a slider which represents the time range from years 2050 to 2100 in real time. Fig. 7 displays the SLR simulation impacting current infrastructure in area number 1, in the year 2100 based on the 8.5 RCP value and the high ice melting scenario; the highest estimation. The simulations in Fig. 8 display the difference in SLR across the edge of the pier in 2060 (Fig. 8a) and 2075 (Fig. 8b). In Fig. 9b and Fig. 9c the sea level in 2095 and 2100 is respectively depicted for area 2. It is estimated that the sea level will be 9 cm above the current ground for 2095 and 19 cm above for 2100. The estimated sea level across the pier edge for the area 2 is showcased in Fig. 10 for 2060 and 2070. The slope of the ground makes the level difference more distinguishable.

(a) (b)

Fig. 7: SLR simulation in area number 1. Existing infrastructure : (**a**) Before. (**b**) After the simulation is activated.

Since the computed values represent offsets from the current sea level, the main prerequisite for the reliable simulation of the level rise is to correctly establish the present sea level in our system. Hololens 2 considers the origin of the coordinate system the device itself, i.e the physical origin of our space is the user's head and the rise simulation becomes relevant to the user's height. We observe that the current sea level is the sum of the device's distance to the ground (pier) and the offset between the pier and the sea surface. Due to lack

(a) (b)

Fig. 8: SLR simulation across the pier edge of area 1 (RCP 8.5, high ice melting scenario). Years: (**a**) 2060. (**b**) 2075.

(a)

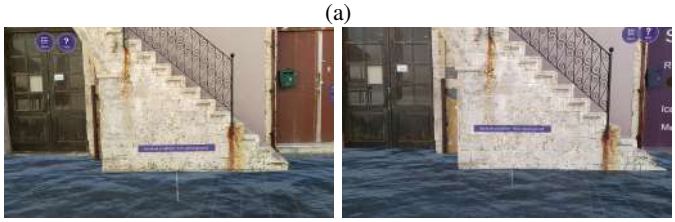

(b) (c)

Fig. 9: SLR simulation in area 2 (RCP 8.5, high ice melting scenario): (**a**) Existing space. (**b**) Year 2095. (**c**) Year 2100.

of available data, we measured the offset between the pier and the sea surface manually on all 3 simulation areas. To measure the device's distance to the ground, a ground detection process was developed based on ray casting. When launching the application a ray is cast and the impact points where it hits the spatial mesh of the environment, are collected. The highest recorded absolute value along the vertical (y) axis, is the ground height. Based on those calculations an information label is enabled displaying the height of the simulated sea level from the ground, as shown in Fig. 11b. A compass was included in the menu for orientation (Fig. 12a) demonstrating geographical awareness gained from the calibration process. It renders on the users hand with the palm up gesture and follows

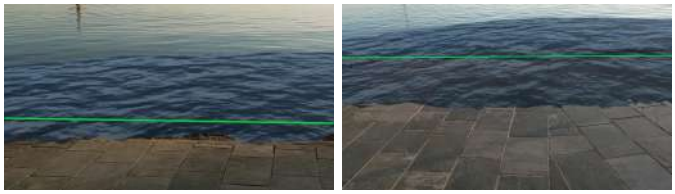

(a) (b)

Fig. 10: SLR simulation across the pier edge of area 2 (RCP 8.5, high ice melting scenario): (**a**) Year 2060. (**b**) Year 2070. The green line indicates the physical pier edge.

it utilizing the device's hand tracking capability. To handle connection loss problems, a reconnect button was added to the menu creating a new TCP client for the AR system to receive GPS information, resulting in uninterrupted application usage without the need for restart.

(a) (b)

Fig. 11: SLR simulation in area 3 (Year 2100, RCP 8.5, high ice melting scenario): (**a**) Before simulation. (**b**) Water simulation. Information label about water height is visible.

(a) (b)

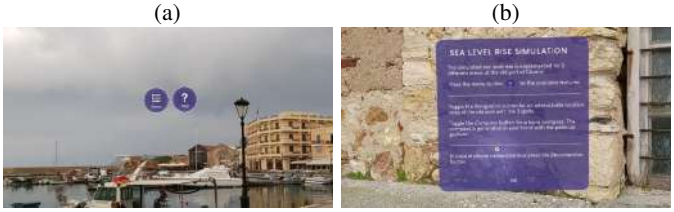

(c) (d)

Fig. 12: (**a**) Compass. (**b**) The features menu. (**c**) The welcome menu. (**d**) Help panel.

IV. Performance

The HoloLens' Device Portal's System Performance tool is used to monitor the application in relation to performance, system demands and how the device technology handles each process. The system diagnostics information are displayed in real time graphs. The pillar of quality factor in a HoloLens application is the frame rate for an optimal user experience. Microsoft recommends a frame rate value at around 60 fps for hologram stability and no less than 30fps for user comfort. While the application is in use for menu panel rendering and user interactions, the frame rate is maintained at 58-60fps. The calibration process and the user scanning configuration also retain these values. Expected frame rate drops appear when the implemented features functionality is commenced. Frame rate values fluctuate between 38-45 fps (Fig. 13) when the navigation feature is enabled, due to the 3D map loading and rendering. The web requests that are performed when the user presses one of the map pins result in a plunge of the frame rate, which reaches around 18-20 fps. These plunges are momentarily as Fig. 13 shows, lasting less than a 1s after

which the frame rate values are immediately restored. When the water shader is rendered, the frame rate values are around 30fps. Environmental conditions are observed to have a slight impact on the frame rate while the water object is rendered. As Hololens 2 is designed mainly for indoor usage, outdoor lighting causes instability. Rendering in sunny spaces drops the frame rate at 25 fps while shadowed areas increased the frame rate at 33fps. Overall, performance was acceptable and interaction was smooth. CPU usage was around 90% with brief drops at around 70% when functionalities were disabled and GPU usage was around 80-90%.

V. Evaluation

In a busy volatile urban area edging with water, we conducted an expert evaluation focusing on the safety of inexperienced users potentially losing spatial awareness. The system was evaluated based on the Think Aloud method [5]. Two experienced computer engineers (both male) carried out the system testing on site and gave their feedback as they went along. We conducted the testing with as much stable lighting conditions as possible. In darker lighting conditions (shadowed areas), both participants had no problem navigating the user interface and interacting with the menu panels. They easily activated the implemented features and considered the water simulation highly immersive. The overall workflow of the application was considered satisfactory, as both users found the embedded instructions on the UI panels helpful. Once they entered bright areas, the user experience was hindered, as the visibility of the interface and the water material was reduced. In order to aid visibility, we darkened the color of the panels and removed any transparency from the panel materials. The water shader remained unchanged since it is highly realistic in optimal circumstances.

Fig. 13: (Up) Frame rate while the navigation feature with the 3D map is enabled (38-45 fps). (Middle) Quick frame rate drop when the user presses a map pin (18-20 fps). (Down) Frame rate when water is rendered ($\sim$ 30 fps).

VI. Discussion and Conclusions

The implemented system presents climate change data via state-of-the-art AR technology, tackling interaction and location awareness challenges. Predicted environmental scenarios were visualized in their actual physical settings. Focusing on coastal urban areas, SLR data were sourced through the MCD, regarding three RCP values (2.6, 4.5 and 8.5). A high and a medium melting scenario were considered in the estimations. The estimations were simulated in three areas at the old port of Chania. GPS data were derived from a commercial smartphone. The two devices were interconnected via TCP network protocols forming a unified system. The interactable 3D visualization of future SLR disseminates environmental information in its physical context provoking environmental action. Georeferencing the Hololens device based on smartphone data enabled the accurate spatial placement of the virtual content. The user scanning configuration before the simulation aided the natural occlusion of the virtual content and enhanced ubiquity. The application properly places digital objects in first-time visited areas, while increasing the quality of the placement with each use due to the device's powerful spatial mapping capabilities. System performance was satisfactory for the dynamic loading and rendering of the water and provided a smooth user experience. Outdoor lighting diminishes the Hololens's tracking stability and limits its scanning distance. Experiments were carried out in cloudy weather, preferably before dusk or at dawn. Bright, sunny weather impairs the user experience. Methods for refinement of the environmental scanning configuration, could compensate for occurrences of outdoor tracking instability. The device's spatial understanding could be aided by the introduction of mesh processing steps for surface hole filling or filtering out incorrect floating scanning. Furthermore, surface identification techniques can assist hologram placement.

Acknowledgment

This study has been financially supported by the National RD Project "ECITO: Effects of climate change in the old city of Chania", which is funded by John S. Latsis, Public Benefit Foundation.

References

[1] Bing maps. Avail. online: https://www.bing.com/maps/.
[2] Bing maps rest services. Avail. online: https://docs.microsoft.com/en-us/bingmaps/rest-services/.
[3] Maps sdk. Avail. online: https://www.microsoft.com/en-us/garage/profiles/maps-sdk/.
[4] Sea level rise. Avail. online: https://www.antarcticglaciers.org/glaciers-and-climate/sea-level-rise-2/.
[5] O Alhadreti and P Mayhew. Rethinking thinking aloud: A comparison of three think-aloud protocols. In *Proc. of the 2018 CHI Conf. on Human Factors in Computing Systems,*1–12, 2018.
[6] R P Allan, E Hawkins, N Bellouin, and B Collins. Ipcc, 2021: Summary for policymakers. 2021.
[7] D F Argus, WR Peltier, R Drummond, and A W Moore. The antarctica component of postglacial rebound model ice-6g_c (vm5a) based on gps positioning, exposure age dating of ice thicknesses, and relative sea level histories. *Geophysical Journal International*, 198(1):537–563, 2014.
[8] M Basyir, M Nasir, S Suryati, and W Mellyssa. Determination of nearest emergency service office using haversine formula based on android platform. *EMITTER Int. J. of Eng. Tech.*, 5(2):270–278, 2017.
[9] D D Cham, N T Son, N Q Minh, N T Thanh, and T T Dung. An analysis of shoreline changes using combined multitemporal remote sensing and digital evaluation model. *Civ. Eng. J*, 6(1):1–10, 2020.
[10] YM Chiou. Multi-party mixed reality interaction for earth sciences education. In *Proc. 13th Int. Conf. on Tangible, Embedded, and Embodied Interaction,*719–722, 2019.
[11] J A Church, N J White, L F Konikow, C M Domingues, J G Cogley, E Rignot, J M Gregory, M R van den Broeke, A J Monaghan, and I Velicogna. Revisiting the earth's sea-level and energy budgets from 1961 to 2008. *Geophys. Res. Lett.*, 38(18), 2011.
[12] A Çöltekin, I Lochhead, M Madden, S Christophe, A Devaux, C Pettit, O Lock, S Shukla, and L Herman. Extended reality in spatial sciences: A review of research challenges and future directions.

[13] A Çöltekin, D Oprean, J O Wallgrün, and A Klippel. Where are we now? re-visiting the digital earth through human-centered virtual and augmented reality geovisualization environments. *Int. Journal of Digital Earth*, 12(2):119–122, 2019.

[14] A Coppens. Merging real and virtual worlds: An analysis of the state of the art and practical evaluation of microsoft hololens. *arXiv preprint arXiv:1706.08096*, 2017.

[15] G Daskalogrigorakis, A McNamara, and K Mania. Holo-box: Level-of-detail glanceable interfaces for augmented reality. In *ACM SIGGRAPH 2021 Posters,*1–2. 2021.

[16] R M DeConto and D Pollard. Contribution of antarctica to past and future sea-level rise. *Nature*, 531(7596):591–597, 2016.

[17] U Engelke, C Rogers, J Klump, and I Lau. Hypar: Situated mineralogy exploration in augmented reality. In *17th Int. Conf. on Virtual-Reality Continuum and Its Applications in Industry,*1–5, 2019.

[18] A Giannakidis, G Giakoumidakis, and K Mania. 3d photorealistic scientific visualization of tsunami waves and sea level rise. In *2014 IEEE Int.Conf.on Imag. Syst. and Techniques Proc.,*167–172. IEEE, 2014.

[19] J M Gregory, S M Griffies, C W Hughes, J A Lowe, J A Church, I Fukimori, N Gomez, R E Kopp, F Landerer, G L Cozannet, et al. Concepts and terminology for sea level: Mean, variability and change, both local and global. *Surveys in Geophysics*, 40(6):1251–1289, 2019.

[20] G Griggs and B G Reguero. Coastal adaptation to climate change and sea-level rise. *Water*, 13(16):2151, 2021.

[21] R L M Guarese and A Maciel. Development and usability analysis of a mixed reality gps navigation application for the microsoft hololens. In *Computer Graphics Int. Conf.,*431–437. Springer, 2019.

[22] J Hinkel, D Lincke, A T Vafeidis, M Perrette, R J Nicholls, R SJ Tol, B Marzeion, X Fettweis, C Ionescu, and A Levermann. Coastal flood damage and adaptation costs under 21st century sea-level rise. *Proc. National Academy of Sciences*, 111(9):3292–3297, 2014.

[23] S Isrie, N Moonen, H Schipper, H Bergsma, and F Leferink. Measuring, logging, and visualizing pulsed electromagnetic fields combined with gps location information. In *2018 Int. Symp. on electromagnetic compatibility (EMC EUROPE),*500–505. IEEE, 2018.

[24] S Jevrejeva, J C Moore, and A Grinsted. Sea level projections to ad2500 with a new generation of climate change scenarios. *Global and Planetary Change*, 80:14–20, 2012.

[25] M Katsiokalis, L Ragia, and K Mania. Outdoors mobile augmented reality for coastal erosion visualization based on geographical data. In *Proc. Int. Workshop on Cross-Reality (XR) Interaction co-located with 14th ACM Int. Conf. on Interactive Surfaces and Spaces (ACM ISS 2020), Lisbon, Portugal, October 8, 2020*, volume 2779 of *CEUR Workshop Proc.* CEUR-WS.org, 2020.

[26] G A Koulieris, K Akşit, M. Stengel, Rł K Mantiuk, K Mania, and C Richardt. Near-eye display and tracking technologies for virtual and augmented reality. In *Computer Graphics Forum,*38(2):493–519, 2019.

[27] S A Kulp and B H Strauss. New elevation data triple estimates of global vulnerability to sea-level rise and coastal flooding. *Nat. Commun.*, 10(1):1–12, 2019.

[28] F F Ling, C Elvezio, J Bullock, S Henderson, and S Feiner. A hybrid rtk gnss and slam outdoor augmented reality system. In *2019 IEEE Conf. on Virtual Reality and 3D User Interfaces (VR),*1044–1045. IEEE, 2019.

[29] B Liu, L Ding, and L Meng. Spatial knowledge acquisition with virtual semantic landmarks in mixed reality-based indoor navigation. *Cartography and Geographic Inform. Sci.*, 48(4):305–319, 2021.

[30] A Melet, R Almar, M Hemer, G Le Cozannet, B Meyssignac, and P Ruggiero. Contribution of wave setup to projected coastal sea level changes. *J. Geophys. Res.: Oceans*, 125(8):e2020JC016078, 2020.

[31] T Menard, J Miller, M Nowak, and D Norris. Comparing the gps capabilities of the samsung galaxy s, motorola droid x, and the apple iphone for vehicle tracking using freesim_mobile. In *2011 14th Int. IEEE Conf. on Intelligent Transportation Systems (ITSC),*985–990. IEEE, 2011.

[32] K Merry and P Bettinger. Smartphone gps accuracy study in an urban environment. *PloS one*, 14(7):e0219890, 2019.

[33] D Molinari, K M De Bruijn, J T Castillo-Rodríguez, G T Aronica, and L M Bouwer. Validation of flood risk models: Current practice and possible improvements. *Int. J. Disaster Risk Reduct.*, 33:441–448, 2019.

[34] I N Monioudi, A F Velegrakis, A E Chatzipavlis, A Rigos, T Karambas, M I Vousdoukas, T Hasiotis, N Koukourouvli, P Peduzzi, E Manoutsoglou, et al. Assessment of island beach erosion due to sea level rise: the case of the aegean archipelago (eastern mediterranean). *Natural Hazards and Earth System Sciences*, 17(3):449–466, 2017.

[35] F Munoz-Montoya, M-C Juan, M Mendez-Lopez, and C Fidalgo. Augmented reality based on slam to assess spatial short-term memory. *IEEE Access*, 7:2453–2466, 2018.

[36] A Panagiotopoulou, L Ragia, and F Sarri. Sea level rise future predictions: a case study in crete. In *Proc. of the 8th Int. Conf. on Geographical Information Systems Theory, Applications and Management (GISTAM 2022),*166-172, 2022.

[37] C Panou, L Ragia, D Dimelli, and K Mania. An architecture for mobile outdoors augmented reality for cultural heritage. *ISPRS Int. Journal of Geo-Inf.*, 7(12):463, 2018.

[38] S Park, S Bokijonov, and Y Choi. Review of microsoft hololens applications over the past five years. *Appl. Sci.*, 11(16):7259, 2021.

[39] W R Peltier, DF Argus, and R Drummond. Space geodesy constrains ice age terminal deglaciation: The global ice-6g_c (vm5a) model. *J. Geophys. Res.: Solid Earth*, 120(1):450–487, 2015.

[40] S Petrakis, G Alexandrakis, and S Poulos. Recent and future trends of beach zone evolution in relation to its physical characteristics: the case of the almiros bay (island of crete, south aegean sea). *Global Nest J*, 16:104–113, 2013.

[41] C Praschl, O Krauss, and G A Zwettler. Towards retooling the microsoft hololens as outdoor ar and mr device. In *17th Int. Conf. on Modeling and Applied Simulation*, pages 126–135, 2018.

[42] C Praschl, O Krauss, and G A Zwettler. Enabling outdoor mr capabilities for head mounted displays: a case study. *Int. Journal of Simulation and Process Modelling*, 15(6):512–523, 2020.

[43] L Ragia, F Sarri, and K Mania. Precise photorealistic visualization for restoration of historic buildings based on tacheometry data. *Journal of Geographical Systems*, 20(2):115–137, 2018.

[44] R Rydvanskiy and N Hedley. Mixed reality flood visualizations: reflections on development and usability of current systems. *ISPRS Int. Journal of Geo-Information*, 10(2):82, 2021.

[45] G Scardino, F Sabatier, G Scicchitano, A Piscitelli, M Milella, A Vecchio, and G Anzidei, M Mastronuzzi. Sea-level rise and shoreline changes along an open sandy coast: Case study of gulf of taranto, italy. *Water*, 12(5):1414, 2020.

[46] S Sela and E Gustafsson. Interactive visualization of underground infrastructures via mixed reality, 2019.

[47] S Shannon, R Smith, A Wiltshire, T Payne, M Huss, R Betts, J Caesar, A Koutroulis, D Jones, and S Harrison. Global glacier volume projections under high-end climate change scenarios. *The Cryosphere*, 13(1):325–350, 2019.

[48] J Stigall, S T Bodempudi, S Sharma, D Scribner, J Grynovicki, and P Grazaitis. Building evacuation using microsoft hololens. In *27th Int. Conf. on Software Engineering and Data Engineering,*8–10, 2018.

[49] J PM Syvitski, A J Kettner, I Overeem, E WH Hutton, M T Hannon, G R Brakenridge, J Day, C Vörösmarty, Y Saito, L Giosan, et al. Sinking deltas due to human activities. *Nature Geoscience*, 2(10):681–686, 2009.

[50] A Toimil, P Camus, IJ Losada, G Le Cozannet, RJ Nicholls, D Idier, and A Maspataud. Climate change-driven coastal erosion modelling in temperate sandy beaches: Methods and uncertainty treatment. *Earth-Science Reviews*, 202:103110, 2020.

[51] F Van Diggelen and P Enge. The world's first gps mooc and worldwide laboratory using smartphones. In *Proc. 28th Int. Tech. Meet. of the satellite division of ION (ION GNSS+ 2015),*361–369, 2015.

[52] Y Wada, L PH Van Beek, F C Sperna Weiland, B F Chao, Y-H Wu, and M FP Bierkens. Past and future contribution of global groundwater depletion to sea-level rise. *Geophysical Research Letters*, 39(9), 2012.

[53] W Wang, X Wu, A He, and Z Chen. Modelling and visualizing holographic 3d geographical scenes with timely data based on the hololens. *ISPRS Int. J. Geoinf*, 8(12):539, 2019.

[54] C Wolff, A T Vafeidis, S Muis, D Lincke, A Satta, P Lionello, J A Jimenez, D Conte, and J Hinkel. A mediterranean coastal database for assessing the impacts of sea-level rise and associated hazards. *Scientific data*, 5(1):1–11, 2018.

[55] P L Woodworth. Differences between mean tide level and mean sea level. *Journal of Geodesy*, 91(1):69–90, 2017.

[56] A Yamashita, K Sato, S Sato, and K Matsubayashi. Pedestrian navigation system for visually impaired people using hololens and rfid. In *2017 Conf. on Technol. and Appl. of Artif. Intell. (TAAI),*130–135. IEEE, 2017.

[57] P A Zandbergen and S J Barbeau. Positional accuracy of assisted gps data from high-sensitivity gps-enabled mobile phones. *The Journal of Navigation*, 64(3):381–399, 2011.